Substituent and Solvent Effects on the Nature of the Transitions of Pyrenol and Pyranine. Identification of an Intermediate in the Excited-State Proton-Transfer Reaction†

T.-H. Tran-Thi,*,‡ C. Prayer,‡ Ph. Millié,§ P. Uznanski,|| and James T. Hynes⊥

Laboratoire de Photophysique et de Photochimie and Groupe de Chimie Quantique, CEA/Saclay, DSM/DRECAM/SPAM and LFP FRE 2298, 91191 Gif-sur-Yvette Cedex, France, Center of Molecular and Macromolecular Studies, PAS Sienkiewicza 112,90-363 Lodz, Poland, Département de Chimie, Ecole Normale Supérieure, CNRS UMR 8640, 24 rue Lhomond, 75231 Paris Cedex 05, France, and Department of Chemistry and Biochemistry, University of Colorado, Boulder, Colorado 80309-0215

Received: July 6, 2001; In Final Form: December 11, 2001

A comparative study of pyrenol and its trisulfonated derivative, pyranine, is undertaken to provide new clues for the understanding of the excited-state proton-transfer reaction (ESPT) of hydroxyarenes (ArOH*). A particular goal is to elucidate the nature of a transient intermediate involved in a three step mechanism of ESPT, as recently revealed in a dynamical study of excited pyranine in water. The present focus is on the reactant side, before the proton transfer occurs, and particular attention is given to the analysis of the nature of the electronic transitions and to the solute−solvent interactions in the ground and excited states of the ArOHs. Using both quantum chemical calculations and solvatochromism analyses, both (a) the role of electron-withdrawing substituents and H-bond interaction with the solvent in stabilizing the two lowest excited states, ^1L_b and ^1L_a, and (b) their relevance to the inversion of these two states are studied. The results allow the identification of the intermediate species in the three step mechanism of the ESPT of excited pyranine in water as a ^1L_a state acid form, with appreciable charge-transfer character, as distinct from the ^1L_b acid form reached in absorption. The results, which differ from more standard pictures of ESPT, are discussed within the perspective of a three valence bond form model for the ESPT process.

I. Introduction

As is well-known, the acidity of hydroxyarenes (ArOH) is considerably enhanced in the excited electronic state.[1] For example, in water solvent, the ArOH acidity can increase by a factor of one to ten million for the excited-state proton-transfer (ESPT) reaction. Such acidity increases are quantified in terms of the pK_a* of ArOH*, which is lowered by six to seven units compared to pK_a for the ground-state acid.[2] Predicted pK_a* values are typically determined through a Förster cycle,[3] which exploits, e.g., absorption measurements of ArOH and ArO^- to establish the $\Delta pK_a = pK_a - pK_a$* value for the acid. Fluorescence measurements of ArOH* and ArO^-* can be used for the same purpose, and indeed most workers determine ΔpK_a as the average of the values inferred from these and absorption measurements.[4] There has been extensive experimental activity on ESPT, especially via ultrafast spectroscopic studies in recent years,[5] with increasing emphasis on the dynamics, rather than the energetics, of this reaction class.

One standard view of ESPT focuses on the issue of the enhanced excited-state acidity, which is supposed to arise from a partial charge transfer, upon excitation, from the lone π pair of the hydroxylic oxygen to the ring; the resulting coulomb repulsion between the $O^{\delta+}$ and the acidic proton would thus increase the acidity.[6,7] The existence of such an intramolecular charge transfer has not, however, been established.[8] Further, this view does not address the molecular mechanism of the ESPT, e.g., the identity of the reaction coordinate, etc., an issue which has received attention for ground-state PT reactions.[9,10]

Another view, essentially decoupled from the one just recounted, focuses on an overall electronic state picture of the ESPT and points to the involvement of inversion of states in the excited state of ArOH, primarily discussed for the case of 1-naphthol (1-NpOH), whose ^1L_b (lowest) and ^1L_a transitions are very close in energy (we use the Platt notation currently adopted for aromatic compounds:[11] the axes *a* and *b* refer to the long and short axes, respectively, of the aromatic ring). In a first perspective,[12] the energy of the two states can appreciably decrease due to strong H-bond interaction between 1-NpOH and some bases (1-NpO−H···B). This decrease is more important for the ^1L_a state, and therefore the energy gap between ^1L_b and ^1L_a is reduced, but ^1L_b (1-NpO−H*···B) remains the lowest excited-state reached in absorption. In fluorescence emission, ^1L_b is the emitting state in weakly polar solvents. However, in more polar solvents, the emission occurs from the ^1L_a state whose configuration corresponds to the proton-transferred form (1-NpO^-*···HB^+), the solvated anion precursor. This $^1L_b/^1L_a$ level inversion is thus associated with the ESPT itself. While the ^1L_a state in the Franck−Condon configuration (but not accessed in the lowest energy transition) is more polar than the ^1L_b state,[13] this level inversion scenario does not directly address why it is that the excited-state acidity is enhanced compared to that of the ground state. The $^1L_b/^1L_a$ level inversion picture has been greatly enriched in important recent studies by Knochenmuss and co-workers[13,14] and in particular the contribution[14] which argues that both the surrounding solvent motion and internal vibronic coupling in 1-NpOH* are critical features in

† Part of the special issue "Noboru Mataga Festschrift".
‡ Laboratoire de Photophysique et de Photochimie.
§ Groupe de Chimie Quantique, SPAM.
|| Center of Molecular and Macromolecular Studies.
⊥ Département de Chimie and Department of Chemistry and Biochemistry.

10.1021/jp0125606 CCC: $22.00
Published on Web 02/07/2002

the inversion process. Nonetheless, the inversion is again associated with the ESPT process itself, and the underlying cause of the enhanced excited-state acidity is not addressed.

In a previous study, several of the present authors have probed the dynamics of the proton-transfer reaction from excited pyranine (3sPyOH) to water molecules with a hundred femtosecond time resolution.[15] It was shown, for the first time, that the proton-transfer reaction in water proceeds via three successive steps, two of which precede the actual proton-transfer event. The first very fast step, less than 300 fs, was attributed to the solvation dynamics of 3sPyOH*. The last, much slower (87 ps), step is the proton-transfer reaction proper, during which is observed the correlated decay of the excited protonated species 3sPyOH* and rise of the conjugate base excited anion $3sPyO^-$*. This last step, which also involves diffusive recombination of the $3sPyO^-$* and H_3O^+ ions, was previously observed, with the same time scale, by Pines et al.[16] The second step (2.2 ps) remains a mystery. Initially, it was tentatively assigned to a specific hydrogen bond formation between the hydroxylic group of 3sPyOH* and a water molecule, involving a dynamical reorganization of the hydrogen-bonded water network linked with this particular water molecule.[15] Another hypothesis was also suggested, which involves the existence of an intermediate to which the locally excited (LE) state of 3sPyOH* relaxes after complete solvation;[17] a three-valence bond (VB) form model was proposed to account for the three step ESPT process, with a suggested intermediate characterized by significant charge transfer.[17,18] In this view, the intermediate— and not the LE state reached in absorption— would have the charge-transfer character envisaged in the first standard view described above; the LE state would be predominantly one VB form, while the CT intermediate could be predominantly the second form. The subsequent ESPT reaction itself would involve PT from this intermediate to the solvent, producing the proton-transferred product, which would be predominantly the final VB form.

In any event, it is this mysterious second step that motivates us not only to try to clarify its character and the intermediate's identity, but also to probe, with a new eye, more traditional ESPT ideas formulated in the past and mentioned above: the existence of an intramolecular charge transfer from the lone pair of the oxygen to the ring and the inversion of states between the protonated and deprotonated forms.

Accordingly, in the present work, our aim is to bring new clues for the understanding of the nature of ESPT, focusing on the intermediate species; thus, our attention is focused here on the reactant side of the ESPT process, *before* any proton transfer occurs. In this connection, there are two important aspects: to elucidate the nature of the electronic transitions of pyranine and to understand the nature of the solute−solvent interactions in the ground and excited states. To these ends, we will compare the optical properties of pyranine and pyrenol, which display very different behavior: pyrenol, in its excited state, does not transfer a proton to water,[17] while pyranine, its trisulfonated derivative, does.[15,16]

To be able to assign the electronic transitions of the studied compounds, we will first compare the optical properties of pyrenol (PyOH) and pyrene (Py) in their ground and excited states. Next, we will study the net effect of the degree of sulfonation (1 SO_3^-, 4 SO_3^-) on pyrene, which possesses the same aromatic skeleton as pyrenol. We will compare these results to the effect of sulfonation on pyrenol (3 SO_3^-) to produce pyranine. For all these compounds (see Figure 1), quantum chemical calculations are performed to provide us both with a guideline for the assignments of the electronic transitions and with qualitative tools for a prediction of the effect of electron-withdrawing substituents on pyrene and pyrenol. To lighten the calculations, carboxylate groups, CO_2^-, are used instead of the SO_3^- groups; since the CO_2^- group displays a similar electron-withdrawing behavior,[19] we expect the energy variation to be of the same order of magnitude for the two substituents, which will allow prediction of the effect of the SO_3^- groups.

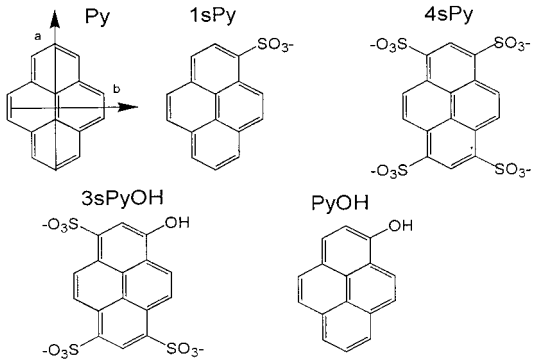

Figure 1. Schematic representation of the compounds studied. The counterions, Na^+, of the three salts (1sPy, 4sPy, and 3sPyOH) are omitted.

To understand the nature of the solute−solvent interaction and to probe the existence of hydrogen bond formation in the ground and excited-state acid forms, we will study the solvatochromism of pyranine and pyrenol, using a series of aprotic solvents and protic ones and varying their capacity for accepting or donating a hydrogen bond. We will also examine the nature of the transitions of pyrenol and pyranine to quantify the extent of charge delocalization of the oxygen π lone pair in the hydroxylic group. Certain other results on the existence of ESPT and spectroscopic aspects of the excited anion are also given to help to provide perspective.

The outline of the remainder of this paper is as follows. After the Experimental Section, section II, which includes a discussion of the quantum chemical methods, the absorption and fluorescence transitions in the primary compounds of interest, PyOH and 3sPyOH, are examined in section III, both spectroscopically and with the aid of quantum chemical calculations, especially in connection with substituent effects. These studies identify the absorbing and fluorescing states in PyOH as a weakly polar ^1L_b state and the absorbing state in 3sPyOH as a moderately polar ^1L_b state. The fluorescing state of 3sPyOH is identified as a polar ^1L_a state via the solvatochromism studies in section IV, and these results are used to identify the intermediate in the 3sPyOH ESPT dynamics in water. The intermediate formation is discussed in the three VB form model perspective in section V, while section VI concludes, focusing on the general implications for the interpretation of ESPT.

II. Experimental Section

Materials. Pyrene (Pyr) 99% and 1-hydroxypyrene (Pyrenol or PyOH) 98% pure from Aldrich were used as received. 1,3,6,8-pyrene tetrasulfonic acid tetrasodium salt (4sPyr) and 8-hydroxy-1,3,6 pyrenetrisulfonic acid trisodium salt (3sPyOH) laser grade were purchased from Kodak. Quinine sulfate dihydrate is from Prolabo. The pyrene monosulfonic acid monosodium salt (1sPy) was synthesized according to the modified method of Tietze and Bayer.[20] Toluene (Uvasol, 99.9%), methanol (MeOH, Uvasol 99.8%), ethanol (EtOH,Uvasol 99.8%), acetonitrile (Uvasol 99.7%, CH_3CN) and dimethylsulfoxyde (Uvasol, 99.8%, DMSO) of spectroscopic grade come from Merck.

Formamide (Fluka 99%, FA), chloroform ($CHCl_3$), 1,2-dichloroethane ($C_2H_4Cl_2$), *N*,*N*-dimethylformamide (DMF, 99.8%), ethylene glycol (EtGOH), and 2,2′,2″ trifluoroethanol (TFE,) from Aldrich, were used without further purification. Water was purified by Milli-ro and Milli-Q systems of Millipore to a resistivity >18 MΩ. cm^{-1}. Sodium hydroxyde (NaOH) and hydrochloric acid (HCl) from Fluka were used to adjust the pH of the solutions.

Steady-State Absorption and Fluorimetry. The UV−vis spectra were recorded with a Perkin-Elmer (Lambda 900). For fluorescence studies, very diluted solutions were used to avoid spectral distortions due to the innerfilter effect and emission reabsorption. The fluorescence and excitation spectra were recorded with a SPEX fluorolog over the UV and visible domain. The excitation source is a 150 W xenon lamp The spectra are corrected for the monochromator and photomultiplier response over the 250−750 nm domain. For the fluorescence quantum yield determinations, we used as standard,[21] the Quinine sulfate dihydrate.

Time-Resolved Fluorimetry. The fluorescence decay times were measured using the Edinburg Instrument 199F time-correlated single-photon- counting system. The excitation source is a dye laser pumped by a frequency doubled Nd:YAG (Quantronix, 76 MHz). With the Rhodamine 6G dye, the excitation wavelength can be tuned from 560 to 620 nm over the visible and from 280 to 310 nm over the blue domain. The fwmh of the laser profile through a scattered solution of pinacyanol (standard compound with short lifetime <100 ps) and the overall instrumentation response time was 180 ps at the excitation wavelength.

Quantum Chemical Calculation Methods. The quantum chemical calculations have been performed in the framework of the semiempirical CS−INDO method.[22] This method has proved successful in studying the electronic states of conjugated molecules.[23] However, for molecules as large as those studied here, the CI calculations have to be restricted to a limited number of configurations and only the main MOs, i.e., the π type MOs are taken into consideration. Consequently, dynamic electronic correlation and repolarization of the sigma system in the excited states are not correctly taken into account. These approximations lead to a preferential stabilization of localized excited states compared to charge-transfer states.[24] To overcome these difficulties, the CS−INDO method was modified. This new scheme, used here, is described in detail elsewhere;[24] the main modification lies in the localization of bonding and antibonding σ MOs. In this way, the correlation and repolarization effects described above can be taken into account without too large CI calculations, and precise results for charge-transfer states[24] or very large molecules[25] can be obtained. Geometry optimizations were performed with the MOPAC package using the AM1 Hamiltonian.[26] The parameters required by the CS−INDO procedure were taken to be identical to those of ref 27. Because of difficulties associated with the hypervalent character of the S atom, SO_3^- groups have been replaced in the calculations by CO_2^- groups, which have similar electron-withdrawing effects. (In the presence of hypervalency, calculated results depend very sensitively on the semiempirical parameters employed, and we consider the available collection of unambiguous spectroscopic results to be too modest to provide reliable semiempirical parameters for the calculation of spectroscopic transitions.)

III. Nature of the Transitions

In succeeding subsections, we characterize the nature and energetics of the absorption and fluorescence transitions of pyrene, pyrenol, and their carboxylate and sulfonate derivatives, concluding with the acid of primary focus: pyranine, 3sPyOH.

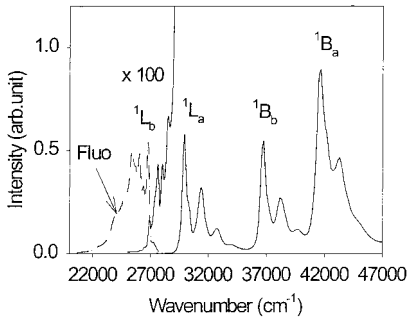

Figure 2. Absorption and fluorescence spectra of pyrene in *n*-hexane.

TABLE 1: Quantum Chemical Calculations of the Energy of the Two Lowest Transitions of Pyrene, Carboxylated Pyrenes, Protonated Pyrenol (PyOH), Tricarboxylated Pyrenol (3(CO_2^-)PyOH)

compound	transitions (cm^{-1})	$(\mu)^2$ (D)	$f(^1L_a)/f(^1L_b)$	permanent μ (D)
				GS: 0
Pyr	$S_0 \rightarrow {}^1L_b$: 27600	0.45	86.2	^1L_b: 0
	$S_0 \rightarrow {}^1L_a$: 32900	38.8		^1L_a: 0
	$S_0 \rightarrow {}^1L_b$: 27050	0.55		
(1CO_2^-)Pyr	$S_0 \rightarrow {}^1L_a$: 31000	47.6	86.5	
	$S_0 \rightarrow {}^1L_b$: 26200	0.81		
(4CO_2^-)Pyr	$S_0 \rightarrow {}^1L_a$: 29400	68.9	85.1	
PyOH	$S_0 \rightarrow {}^1L_b$: 26700	5.20		GS: 2.07
	$S_0 \rightarrow {}^1L_a$: 31400	43.6	8.4	^1L_b: 1.96
				^1L_a: 2.11
(3CO_2^-)PyOH	$S_0 \rightarrow {}^1L_b$: 25800	6.70		
	$S_0 \rightarrow {}^1L_a$: 29200	55.65	8.3	

$(\mu)^2$ is the corresponding transition dipole moment; *f* is the oscillator strength and permanent dipole moment of the ground (GS) and excited states.

III.1. Pyrene (Py). Pyrene spectroscopy has been intensively studied by many groups in the past, and the assignment of the transitions is now well-established.[28] Thulstrup et al.[29] provide a good summary of these investigations that we here briefly recall and compare with our present calculations. The absorption spectrum of pyrene is composed of four transitions (see Figure 2), whose properties are summarized in Table 1 and Table 2.

Pyrene has D_{2h} symmetry. The calculated configurations HOMO (−1) → LUMO and HOMO → LUMO (+1) have the same symmetry, B_{2u}, and due to their proximate energy levels interact together to give the resulting ^1L_b and ^1B_b states. In the ^1L_b state, the transition moments of the two configurations B_{2u} are practically equal and have opposite sign. The resulting transition moment is therefore close to zero and the $S_0 \rightarrow {}^1L_b$ transition is quasi-forbidden. However, the $S_0 \rightarrow {}^1L_b$ transition borrows its intensity by vibrational coupling of ^1L_b with the proximate ^1L_a state. Due to that coupling, the absorption and fluorescence spectra display complex vibrational structures (see Figure 2) whose intensities are strongly sensitive to the substitution and the nature of the environment. Such vibronic coupling is known for other molecules, i.e., triphenylene,[29] naphthalene, and pyrazine,[30] which display a lowest quasi-forbidden transition lying close in energy to a strongly allowed one. As expected for a forbidden transition, the fluorescence lifetime of pyrene, corresponding to $^1L_b \rightarrow S_0$, is long (382 ns in cyclohexane,[31] 199 ns in DMSO[32]).

Both calculations also indicate the existence of other singlet → singlet transitions, but they are symmetry forbidden. According to the calculations of Thulstrup,[29] the allowed transitions to ^1L_b, ^1L_a, ^1B_b, and ^1B_a correspond to ($S_0 \rightarrow S_1$), ($S_0 \rightarrow S_2$), (S_0

TABLE 2: Pyrene Derivatives: Nature and Oscillator Strength of the Transitions and Properties of the Fluorescent State

compound	solvent	ν(abs) (cm^{-1})	$f(^1L_a)/f(^1L_b)$	ν(fluo) (cm^{-1})	$\tau_{f\,(ns)}$	Φ_f
Py	3-methylpentane	^1L_b: 26800 ^1L_a: 29500 ^1B_b: 36200 ^1B_a: 41000	120	^1L_b: 26800	480 ± 70	0.6−0.65
1sPy	H_2O	^1L_b: 26660 ^1L_a: 28700		^1L_b: 26610	64 ± 5	0.85
4sPy	H_2O	^1L_a: 26740		^1L_a: 25970	12.5 ± 0.5	0.56
	DMF	^1L_a: 26660		^1L_a: 26320		
PyOH	H_2O (pH=4)	^1L_b: 26080 ^1L_a: 28960 ^1B_b: 36090 ^1B_a: 41480	8.6	^1L_b: 25910	16.1 ± 0.5	
3sPyOH	H_2O(pH=2)	^1L_b: 24780 ^1L_a: 26070		^1L_a: 22600	4.8 ± 0.5	∼1*
3sPyO-	H_2O(pH=10)	S_1: 21700		S_1: 19450	5.3 ± 0.1	∼1[a]

[a] In water, deprotonation occurs and the fluorescence quantum yield measured corresponds to the sum of the acid and conjugated anion fluorescence.

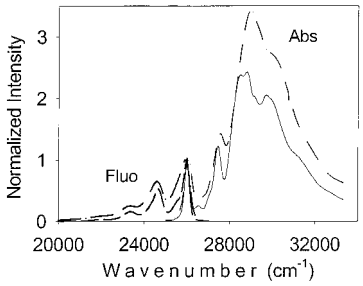

Figure 3. Absorption and fluorescence spectra of PyOH. In water: absorbance (− · ·), fluorescence (− · −). In toluene: absorbance (—), fluorescence (− −). The intensity is normalized to the lowest transition.

→ S_7), and (S_0 → S_{10}), respectively. Our present calculations match quite well with Thulstrup's findings. Both calculations for the isolated molecule give higher values for the energies of the transitions as compared to the experimental data in solution (compare Tables 1 and 2), but they both reproduce quite well the experimental results for the ratio of the oscillator strengths of the corresponding transitions.

III.2. Pyrenol (PyOH). Substitution of an –OH group on the pyrene ring affects the electronic states of the molecule in many ways. First, the D_{2h} symmetry is lost in PyOH and is replaced by a lower one, C_s. We retain the Platt notation to label the transitions of PyOH, the order of which should not be affected by the symmetry loss. The quantum chemical calculations indicate that the energies of the HOMO → LUMO(+1) and HOMO(−1) → LUMO configurations are lower for pyrenol than for pyrene. The two configurations, still close in energy, interact to give the two states ^1L_b and ^1B_b. However, in contrast to the pyrene case, the transition moments of the two A′ configurations have different weights in the ^1L_b state of pyrenol, and therefore the resulting lowest energy transition $S_0 \rightarrow {}^1L_b$ is allowed (see Figure 3 and Table 2).

Vasak et al.[33] have used the magnetic circular dichroism technique to identify the vibronic features of the lowest electronic transition ($S_0 \rightarrow {}^1L_b$) of pyrenol, which is composed of four vibrational bands (see Figure 3). These vibrational bands are much less complicated than those observed for the Py ($S_0 \rightarrow {}^1L_b$) transition. Since the energy gap $\Delta E = E(^1L_a) - E(^1L_b)$ is practically the same for Py and PyOH ($\Delta E_{calc} \sim 5000 \pm 300$ cm^{-1}, $\Delta E_{exp} \sim 2800$ cm^{-1}), this indicates that if there were any vibronic coupling between the two lowest ^1L_b and ^1L_a states, the coupling would be negligible for PyOH as compared to that for Py.

The fluorescence band, which is composed of clearly structured vibrational bands, is the mirror image of the low energy band tail of the wide absorption band (cf. Figure 3). This absorption band corresponds in fact to the sum of two transitions, as demonstrated by Vasak et al.[33] in their magnetic circular dichroism experiment. The oscillator strength corresponding to the absorption transition to ^1L_b in PyOH is much greater than the one observed for Py (see Figure 2 and Table 2). As a consequence of the increase of the oscillator strength of the reverse transition ($^1L_b \rightarrow S_0$), the fluorescence lifetime is much shorter for pyrenol than for pyrene (cf. Table 2).

The permanent dipole moments of the ^1L_b and ^1L_a states of pyrenol have been calculated (see Table 1). In contrast to Py for which the dipole moments of the ground, first, and second excited states are zero, the dipole moment of the PyOH ground state is finite ($\mu = 2.07$ D) but there is no noticeable change of the polarity of the excited states, 1.96 and 2.11 D for ^1L_b and ^1L_a, respectively. Note that the calculations predict quite well the energy of the lowest transition ^1L_b and the ratio of the oscillator strengths of $S_0 \rightarrow {}^1L_b$ and $S_0 \rightarrow {}^1L_a$ (compare Tables 1 and 2). The calculated gap between the two transitions is however higher (4700 cm^{-1}) than the experimental value in water (2880 cm^{-1}). We will discuss the above in connection with solvatochromism studies in section IV.

III.3. Effect of the Substituents on the Nature and Energy of the Transitions of Pyrene. *III.3.1. Effect of the Carboxylate Substituents: Calculation Predictions.* To ease the calculations, SO_3^- was replaced by the CO_2^- substituent, which displays a similar electron-withdrawing effect (cf. section II). The calculations in Table 1 indicate that substitution of one CO_2^- group lowers the energy of both pyrene states, but to a much greater extent for ^1L_a (1900 cm^{-1}) than for ^1L_b (550 cm^{-1}). However, this effect is not additive: in the presence of four CO_2^- groups, ^1L_a and ^1L_b are lowered by 3500 and 1400 cm^{-1}, respectively. Note from Table 1 that the oscillator strength of the two transitions gradually increases with increasing number of substitution, but that their ratio ($^1L_a/^1L_b$) remains the same, approximately a factor 86. With the hypothesis that SO_3^- groups would provide the same energy-lowering effect, we next attempt to predict the energy of the states of 1sPy and 4sPy from the experimental values of the ^1L_b and ^1L_a states of Py.

III.3.2. Effect of the Sulfonate Substituents (1sPy and 4sPy). The use of the CO_2^- calculations predicts, for the SO_3^- substituent effects, that for 1sPy, ^1L_b will lie at 26250 (=26800−550 cm^{-1}) and ^1L_a at 27600 cm^{-1} (=29500−1900 cm^{-1}). The experimental values (cf. Table 2) are quite close to these

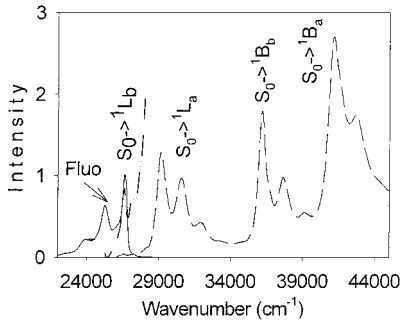

Figure 4. Absorption and fluorescence spectra of 1sPy in water: absorbance (− −), absorbance ×20 (− · ·), fluorescence (—).

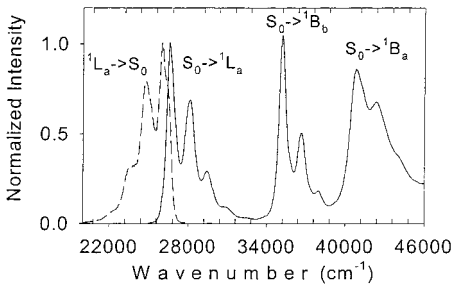

Figure 5. Absorption and fluorescence spectra of 4sPy in water. The intensity is normalized to the lowest transition.

predictions, though slightly larger, 26600 and 28700 cm^{-1}, respectively. The calculations also predict that ^1L_b of 1sPy will remain weakly allowed (see Table 1).

The absorption and fluorescence spectra of 1sPy are quite similar to those of PyOH though in the present case the lowest transition attributed to $S_0 \rightarrow {}^1L_b$ is less allowed. This is in agreement with the predictions of the calculation and also with the radiative lifetime, 64 ± 5 ns in water, which is 4 times longer than that of PyOH (see Figures 2 and 3 and compare Figures 1 and 2).

With the tetrasulfonated 4sPy compound, the D_{2h} symmetry of Py is recovered. Based on the Py properties, we would expect for 4sPy a weakly allowed ^1L_b transition. Further, with our working hypothesis that the effect of the four SO_3^- would be similar to four CO_2^-, we would expect a lowering of the energy of the^1L_b and ^1L_a transitions of 1400 and 3500 cm^{-1}, respectively. These considerations would suggest that the two transitions would be very close in energy, 25400 and 26000 cm^{-1} for ^1L_b and ^1L_a, respectively. The experimental value found for the lowest transition of 4sPy is 26740 cm^{-1} (cf Table 2), which is very close to either of the estimated values. This result does not, however, allow us to identify S_1 and further considerations are required, as now discussed.

On the basis of the common D_{2h} symmetry of 4sPy and Py, one might expect the lowest transition to be ^1L_b and accordingly to be only weakly allowed. However, comparison of Figures 2 and 5 shows that, in fact, the absorption (and fluorescence) spectra of 4sPy and Py are totally different in shape and the 4sPy lowest transition is evidently strongly allowed. The fluorescence properties of 4sPy corroborate the absorption findings: the radiative lifetime of 4sPy is considerably shortened as compared to Py (see Table 2), which is indicative of a strongly allowed transition.

On the basis of these considerations, we assign the lowest 4sPy absorption transition (composed of four vibrational bands) to the $S_0 \rightarrow {}^1L_a$ transition. The weakly allowed ^1L_b transition would in this case be hidden by the strongly allowed ^1L_a transition. The lowering effect of the four sulfonate groups is evidently so important in 4sPy that ^1L_a has become the state reached in the lowest transition in absorption and is also the fluorescing state.

To summarize, the calculations of the CO_2^--lowering effect have been successfully applied to predict the energy of the transitions of 1sPy and 4sPy. They allow the predictions that (i) the energy-lowering effect of the SO_3^- is more important for the ^1L_a than for the ^1L_b state, (ii) the energy lowering is not proportional to the substituent number, and (iii) 4 SO_3^- groups can invert the order of the two lowest ^1L_a and ^1L_b transitions. We will now apply the same method to predict the energy of the transitions of 3sPyOH, given the corresponding transitions of PyOH.

III.4. Effect of the Substituents on the Nature and Energy of the Transitions of PyOH and 3sPyOH. *III.4.1. Effect of the Carboxylate Groups: Calculation Predictions.* We now turn to the comparison of the two acids PyOH and 3sPyOH. From Table 1, the comparison of PyOH and ($3CO_2^-$)PyOH shows that the energy levels of the ^1L_b and ^1L_a transitions of PyOH are lowered by 900 and 2200 cm^{-1} respectively, in the presence of three CO_2^- groups. Again, using the calculated CO_2^- substituent effects as a guide, we predict that three SO_3^- substituents should bring the ^1L_b and ^1L_a down to 25180 cm^{-1} ($=E_{1L_b}$(PyOH) − 900 cm^{-1}) and 26760 cm^{-1} ($=E_{1L_a}$(PyOH) − 2200 cm^{-1}), respectively. Therefore, the estimation predicts that the transition to the ^1L_b state will remain the lowest transition in 3sPyOH and the two ^1L_b and ^1L_a states will be separated by ∼1600 cm^{-1}.

III.4.2. Effect of the Sulfonate Groups. The experimental value corresponding to the lowest transition of 3sPyOH in water is 24780 cm^{-1}(see Table 2), which is close to the value of 25180 cm^{-1} just predicted for $S_0 \rightarrow {}^1L_b$. Note that the experimental value was determined for 3sPyOH in a strongly interacting aqueous environment, while the predicted value from calculations is more appropriate for 3sPyOH in a non- or weakly interacting solvent. We will offer further support for this identification and its validity in solvents other than water in section IV.2.

We have just identified the lowest transition of 3sPyOH absorption as $S_0 \rightarrow {}^1L_b$. One would ordinarily expect this ^1L_b state to be the fluorescing one. This expectation is strengthened by the fact that the oscillator strength of the ^1L_b state of 3sPyOH in absorption is greatly enhanced as compared to PyOH (see Figure 6).[34] However, the fluorescence band is *not* in fact the mirror image of the absorption band in any of the solvents studied (see Figure 6). This feature raises the question of the nature of the fluorescing state; though the loss of mirror symmetry can have several origins, such as change of electronic state, a strong overlap of two transitions over a wide absorption band or a change of geometry of the molecule during its excited-state lifetime, we will argue that it is evidently not the ^1L_b state which here fluoresces. A clue for the identification is given by the fact that the shape of the fluorescence band varies as the mirror image of the high energy transition in all solvents (see Figure 6). A consistent explanation would thus be an inversion of the ^1L_b and ^1L_a states,[12−14] during an evolution of the ^1L_b state reached in absorption. To probe this hypothesis and to identify the 3sPyOH* fluorescing state, we have studied the solvatochromism of 3sPyOH and PyOH, as now described.

IV. Solvatochromism of PyOH and 3sPyOH and Identification of the Intermediate in 3sPyOH ESPT in Water

IV.1. PyOH. The absorption and fluorescence spectra of pyrenol, PyOH, are recorded in the three solvents, $CHCl_3$,

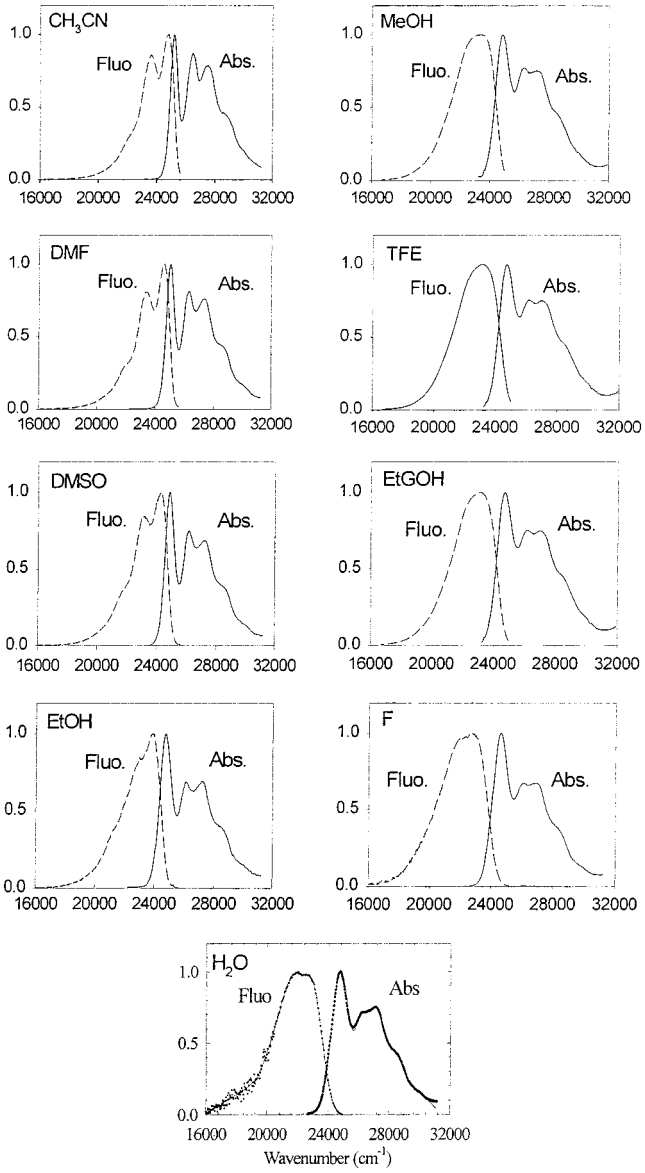

Figure 6. Absorption and fluorescence spectra of 3sPyOH in various solvents. CH_3CN = acetonitrile, DMF = dimethylformamide, DMSO = dimethyl sulfoxide, EtOH = ethanol, MeOH = methanol, TFE = 2,2,2-trifluoroethanol, EtGOH = ethyleneglycol, and F = formamide. The position of the maxima of absorption and fluorescence bands are reported in Table 3

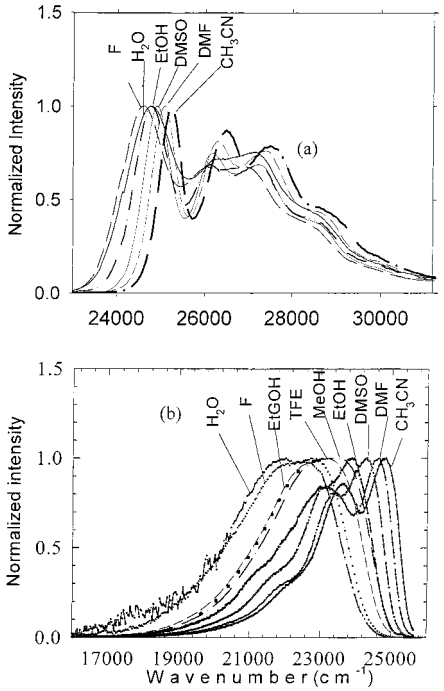

Figure 7. Solvatochromism of 3sPyOH acid form in various solvents: (a) absorption and (b) fluorescence spectra CH_3CN = acetonitrile, DMF = dimethylformamide, DMSO = dimethyl sulfoxide, EtOH = ethanol, MeOH = methanol, TFE = 2,2′,2″ trifluoroethanol, EtGOH = ethyleneglycol, F = formamide, and H_2O = water, pH = 1. In acidic water at pH = 1, the fluorescence spectrum displays both the acid and anion fluorescence bands. Therefore, the fluorescence of the acid form is obtained by subtracting the contribution of the anion fluorescence band, which is well-defined in alkaline solution at pH 10. To avoid congestion, the absorption spectra of 3sPyOH in MeOH, TFE and EtGOH are not included. The maxima of the absorption bands are reported in Table 3.

toluene, and water (see Figure 3 and Table 2). As expected from the quantum chemical calculations on PyOH which predict that the dipole moments in the ground state and in the ^1L_b state are small and very similar, 2.07 and 1.96 D (see Table 1), respectively, the solvatochromism of the ^1L_b state of PyOH is negligible.[35] For example, the maximum Stokes shift between absorption and fluorescence observed for the ^1L_b state in chloroform and water is negligible, 170 cm^{-1}.

Although not the lowest state for either absorption or fluorescence for PyOH, the ^1L_a state characteristics will also prove to be of interest. Similarly to the case of ^1L_b, we observe a small blue shift of the ^1L_a state, 350 cm^{-1}, when going from toluene to water. This result is in general agreement with the calculations which predict that the dipole moments of the ^1L_a and ^1L_b states of the isolated molecule are practically the same, 1.96 and 2.11 D, respectively. On the other hand, one can note that for a protic solvent such as water, the absorption bands corresponding to the ^1L_b and ^1L_a transitions are significantly broadened (see Figure 3), which is indicative of an important solute−solvent interaction, probably through hydrogen bonding. There are two possible sites for H-bond interaction on the hydroxylic group, through the lone pair of the oxygen and the proton. In the excited state, if there were an increase of the charge transfer from the lone pair of the oxygen to the ring, this effect would weaken the first H-bond and strengthen[7,36] the second one, respectively. The combination of these two effects could explain why the observed blue shift is small, despite the significant broadening indicative of a pronounced coupling to the solvent. The former effect would lead to a blue shift and the second to a red shift. These opposite induced effects, combined with the overall decrease of the polarity of the excited-state molecule due to a partial delocalization of the oxygen lone pair into the ring, could result in a small blue shift.

IV.2. 3sPyOH. Figure 6 displays the spectral evolution of the absorption bands with the solvent. Since the shape of the absorption band remains the same independent of the solvent, we continue to attribute the lowest transition to $S_0 \rightarrow {}^1L_b$. Evidently, the energy-lowering effect of three sulfonate groups has brought the two ^1L_b and ^1L_a states close to each other, with a difference of approximately 1300 cm^{-1} (cf section III.4), but it is not sufficient to invert the two states in absorption, as was observed to occur with 4sPy in section III.2. In the following, we focus our attention solely on the solvatochromism of absorption to ^1L_b, which is clearly identifiable as the lowest energy absorption peak for each solvent in Figure 7 (At higher energies, the absorption band is an unknown combination of ^1L_b and ^1L_a and cannot be simply analyzed).

TABLE 3: Kamlet and Taft Parameters for Various Solvents and Peak Absorption and Emission Frequencies of 3SPyOH[a]

no.	solvent	π^*	α	β	absorption (cm^{-1})	fluorescence (cm^{-1})
1	CH_3CN	0.75	0.19	0.40	25030	24810
2	DMF	0.88	0	0.69	25050	24660
3	DMSO	1.00	0	0.76	24890	24290
4	EtOH	0.54	0.83	0.75	24760	23900
5	MeOH	0.60	0.93	0.66	24810	22830
6	F	0.97	0.71	0.48	24580	22830
7	TFE	0.73	1.51	0.00	24880	22960
8	EtGOH	0.92	0.83	0.52	24650	22730
9	H_2O	1.09	1.17	0.47	24780	22600

[a] Values of π^*, α, and β come from ref 39.

The solvatochromism of 3sPyOH differs in many aspects from that of PyOH. A bathochromic (red) shift of the 3sPyOH absorption band is observed when the solvent polarity increases: this is in strong contrast to the PyOH absorption where a small blue shift was observed in section IV.1. A simple charge transfer from the lone pair of the hydroxylic group to the ring would have instead induced a hypsochromic (blue) shift (as was observed for PyOH). Nor can the intrinsic effect of the sulfonated groups, i.e., for 4sPy, account for the shift. A very small blue shift was observed (80 cm^{-1}) for 4sPy when going from a less polar solvent, DMF, to water; therefore, a simple effect of the sulfonate groups cannot induce a red shift.

These considerations suggest that the explanation for the red shift in 3sPyOH absorption is related to a cooperative effect involving both the charge transfer from the oxygen to the ring *and* the sulfonate groups. If the charge transfer from the lone pair of the oxygen were transferred through the ring to one or more electron-withdrawing SO_3^- substituents, the charge-transfer character will be stabilized in polar solvents, leading to a bathochromic shift. Therefore, we tentatively assign the bathochromic shift of the absorption band with increased solvent polarity to an enhanced charge-transfer character in ^1L_b, when going from PyOH to 3sPyOH.

This interpretation can be further pursued noting from Figure 7 and Table 3 that the absorption red shift is enhanced when the solvent is at the same time polar and protic, i.e., for EtOH, MeOH, EtGOH, TFE, water, and F. This suggests that H-bonding is important in the red shift. Further, as was also the case for PyOH, a broadening of the absorption band is observed for the protic solvents, which again suggests the importance of hydrogen bond formation between the solute and solvent. For 3sPyOH as compared to PyOH, there is an extra site for H-bond interaction through the SO_3^- groups. For 3sPyOH, if the charge transfer occurred from the lone pair of the oxygen to one or more sulfonated groups through the ring, it would induce a 2-fold effect; first, as the oxygen atom becomes more positive, the bond between the H and O atoms of the hydroxylic group would weaken. An immediate consequence would be the strengthening of the H-bond between this H atom and a solvent molecule nearby displaying an H-bond-accepting character. Second, because the SO_3^- groups have gained some extra negative charge, the H-bond interactions between these SO_3^- groups and protic solvents with H-bond donor ability will be strengthened. (Note that the charge gain on one or more SO_3^- groups would not be important enough to induce a re-protonation of the SO_3^- site. Such reprotonation still does not occur at negative pH (pH = -0.875).[37]

The solvatochromism of the 3sPyOH fluorescence bands displays a quite different behavior from that of absorption (see Figure 7). There is again a red shift, but it is important to note that it is much larger in fluorescence than in absorption. Further, the fluorescence band is not the mirror image of the $S_0 \rightarrow {}^1L_b$ absorption band (see Figure 6). In most cases, the loss of the mirror symmetry occurs when two or many transitions are buried in a same absorption band and only the lowest one corresponds to the fluorescing state (see for instance pyrene in section III.1). Another origin would be a drastic change of the geometry of the molecule in the excited state, i.e., a torsional motion of the C−C bond in the bianthryl molecule (or other TICT molecules) inducing a huge change in the electronical configuration.[38] This last scenario cannot occur for pyranine which does not display such a bond. Instead, the shape of the fluorescence band varies in the same way as that of the high energy transition ^1L_a, over the 26000−27000 cm^{-1} domain in absorption (cf Figure 7). For instance, the vibrational features persist in both absorption and fluorescence for the less polar solvents (CH_3CN, DMF, and DMSO), while they disappear for the protic solvents. Ethanol displays an intermediate behavior, with the vibrational features still present but strongly broadened. Evidently, the fluorescing state is no longer the ^1L_b state and an inversion has occurred for all the solvents examined.

The state inversion behavior just hypothesized could be understood in terms of the energy-lowering effect on the ^1L_b and ^1L_a states due to the three sulfonated substituents, combined with a lowering effect of strong hydrogen bond formation, as follows. In section III.4, we have shown that the presence of the three sulfonated groups strongly lowers the energy of the 3sPyOH ^1L_a state as compared to the ^1L_b state, so that the two transitions are now very close in energy in absorption. Further, if ^1L_a is characterized by larger CT character than is ^1L_b, the two types of stabilizing H-bond interaction with the H of OH and one or more of the SO_3^- groups, would be enhanced. Evidently, some type of solvent rearrangement has to occur between absorption (to^1L_b) and fluorescence (from^1L_a).

The inversion picture just presented for 3sPyOH and the ^1L_a identity of the fluorescent state could in principle be confirmed by polarization studies in a glassy matrix.[33] Unfortunately, this is not possible for 3sPyOH and we will pursue a solvatochromic route instead. In particular, the proposed inversion should be consistent with the absorption and (enhanced) fluorescence red shifts described above and the evident special importance of H-bonding in protic solvents. To probe this consistency and to reveal more clearly the nature of the markedly enhanced solvent−solute interaction in the ^1L_b and ^1L_a states, we will now exploit the empirical solvatochromic scale of Kamlet and Taft.[39]

IV.3. Kamlet and Taft Analysis of the Solvatochromism of 3sPyOH. Many empirical solvent polarity scales or H-bonding capability scales have been established in the past. A recent Pines group paper[40] on the solvatochromism of 3sPyOH, which advocates 3sPyOH as a useful molecular probe for polar or very acidic environments, compares these various solvent scales available in the literature, including the Kamlet−Taft analysis.[39] In contrast to many empirical scales, which focus only on the solvent's polarity or its H-bonding capability, the Kamlet and Taft[39] scale has provided, for a wide variety of molecules, a quantitative estimation of the contribution of state energy differences of the polarity (π^*) with a polarizability correction term (δ), the H-bond-donating ability (α) and H-bond-accepting ability (β) of the solvent. In such studies, the relation

$$\nu = \nu_0 + s(\pi^* + d\delta) + a(\alpha + b\beta) \qquad \text{(I)}$$

is used to characterize the respective weights *s*, *d*, a, and *b* of contributions of π^*, δ, α, and β. Here ν is the frequency

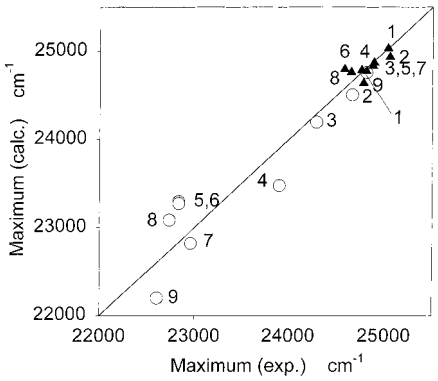

Figure 8. Plot of the calculated maxima of absorption (or fluorescence) as a function of the corresponding experimental maxima for various solvents. The calculated maxima are obtained from the multiparameter fit, using eq I. The line represents a perfect fit for which calculated and experimental values would be equal and each circle represents the fitted value of the absorption (or fluorescence) maximum for a given solvent. From these two multiparameter-fits in absorption and fluorescence, we obtained values of the ν_0 and the weight *s*, a, and *b* of the solvent parameters π^*, α, and β, respectively. *R* is the residual of the multiparameter fit. For absorption: $\nu_0 = 25460 \pm 340$ cm^{-1}, $a(\alpha) = -270 \pm 120$, $s = -290 \pm 270$, $b(\beta) = -380 \pm 270$, and $R = 0.714$. For fluorescence: $\nu_0 = 27000 \pm 1060$ cm^{-1}, $a(\alpha) = -1890 \pm 380$, $s = -1820 \pm 840$, $b(\beta) = -1300 \pm 830$, and $R = 0.925$.

corresponding to the maximum of the lowest electronic transition (red peak of absorption or blue peak of fluorescence) in a given solvent while ν_0 corresponds to the condition where no intermolecular interaction occurs. ν_0 is usually very close to the gas-phase value or that calculated for the "isolated molecule". In the Kamlet and Taft scale, δ is equal to zero for the non-chlorinated aliphatic solvents[39] employed in the present work, so that eq I is reduced to three parameters, π^*, α, and β.

Figure 8 displays the plot of the calculated maxima of absorption or fluorescence as a function of the corresponding experimental values (cf. Table 3) for various solvents. The calculated maxima are obtained from the multiparameter fit, using eq I. The line represents a perfect fit for which calculated and experimental values would be equal and each triangle (or circle) represents the fitted value of ν for a given solvent. From these two multiparameter fits in absorption and fluorescence, we obtained values of the ν_0 and the weight s, a and b of the solvent parameters π^*, α, and β, respectively.

Three important points can be noted. First, the maxima of absorption are grouped around a mean value of 24600 ± 200 cm^{-1} while the fluorescence maxima are spread over a wide wavenumber range ($\sim$3000 cm^{-1}). The solvatochromism is thus much more important in fluorescence than in absorption, consistent with emission from ^1L_a state of greater charge-transfer character than the ^1L_b state reached in absorption. Second, the two fits give a much higher value of ν_0 in fluorescence than in absorption, just as one would expect for a state inversion. For absorption, ν_0 is equal to 25460 ± 340 cm^{-1} and should correspond to the $S_0 \rightarrow {}^1L_b$ transition. This value is in fact very close to the predicted $S_0 \rightarrow {}^1L_b$ transition for the "isolated" 3sPyOH (25180 cm^{-1}). For fluorescence, ν_0 is equal to 27000 ± 1060 cm^{-1} and should correspond to the "isolated" 3sPyOH $^1L_a \rightarrow S_0$ transition. This latter value was predicted to be 26760 cm^{-1} (cf. section III.4.2), which is also in very good agreement with the present data. This is strong support for the ^1L_a identification. Third, in both absorption and fluorescence, the polarity as well as the H-bond-donating and -accepting properties of the solvent contribute to the stabilization of the excited state. However, this effect is much more pronounced on the fluorescence side, as shown by the much higher weights of the solvent parameter, $s(\pi^*) = -1820 \pm 840$, $a(\alpha) = -1890 \pm 380$, and $b(\beta) = -1300 \pm 830$ as compared to the corresponding values on the absorption side, $s(\pi^*) = -290 \pm 270$, $a(\alpha) = -270 \pm 120$, and $b(\beta) = -380 \pm 270$ (Figure 8). This is indicative of a larger charge transfer in ^1L_a than that in ^1L_b. In further support of this, we note that the Stokes shift values are as high as those observed for dye molecules which have a significant charge-transfer character in the excited state.

Pines' findings,[40] using the Kamlet and Taft scale, are in general agreement with ours, for example, showing similar influence of the solvent parameters π^*, α and β on the fluorescence spectra of the acid form. (In ref 39, the solvents studied were non-chlorinated aliphatic solvents for which the polarizability correction term δ is equal to zero, with the exception of pyridine, whose δ value is equal to 1. However, these authors did not give the ν_0 value of the fit or address the nature of the transitions involved in absorption and fluorescence or any possible state inversion. We have taken their set of fluorescence maxima (with the exception of pyridine solvent, which is a base) and fit them as a function of the solvent parameters with eq I to give $\nu_0 = 27970 \pm 820$ cm^{-1}, $a = -1990 \pm 260$, $b = -1800 \pm 550$, and $s = -2040 \pm 650$ and $R = 0.930$. These values are very close to ours within the standard error. In particular, the ν_0 value (27970 ± 820 cm^{-1}) is also very high. (Unfortunately, the data on absorption maxima for the same set of solvents are not available, so that we cannot compare our ν_0 values in absorption.).

From the above analysis of the solvatochromism of both absorption and fluorescence bands of 3sPyOH, we can confidently conclude that the lowest state in absorption is ^1L_b, while the fluorescing state is ^1L_a. The energy lowering of the latter state is strongly solvent dependent. From the less interacting solvent, CH_3CN, to the most interacting one, H_2O, the energy of the ^1L_a state is lowered by 2210 cm^{-1} on the fluorescence side (Table 3), as compared to 470 cm^{-1} on the absorption side (^1L_b). As noted above, the π^*, α, and β contributions are greatly enhanced in fluorescence as compared to absorption (see Figure 8). We now argue that this indicates a charge redistribution in ^1L_a, similar to, but more pronounced than that described for ^1L_b, namely, the charge transfer from the oxygen in OH lone pair through the ring to one or more sulfonate groups that we anticipated in section IV.2. The first aspect of this—connected directly to the sulfonate groups—is supported by the increased importance of the α, solvent H-bond donating, parameter (Table 3), which would be expected for increased negative charge on a sulfonate group. It is noteworthy in this connection that TFE, a solvent which has no H-bond-accepting ability but which displays the highest H-bond-donating ability (and medium polarity), contributes to the stabilization of the excited state as strongly as does water. In addition, the enhanced importance of the solvent H-bond-accepting parameter β for fluorescence, though less pronounced than that of α, would be consistent with the second aspect of the increased charge-transfer character of the ^1L_a state: an increased positive charge on the oxygen of OH.[36] The latter would increase the hydrogen-bonding strength between the repelled H of the hydroxylic group and a H-bond-accepting solvent molecule.

We emphasize that, in the above discussion, the ^1L_a state of 3sPyOH remains a nonproton-transferred acid form. The experimental distinction between it and the excited proton-transferred, ionic form $3sPyO^-*$ is summarized in Table 2, in connection with which ground state $3sPyO^-$ is produced in

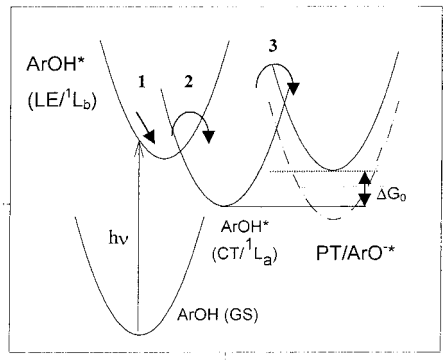

Figure 9. Schematic representation of the three-VB form model for the ESPT process of ArOH*. The locally excited LE is the first-VB form and corresponds to the ^1L_b state accessed in absorption. CT is the second-VB form characterized by a significant charge-transfer character and corresponds to the ^1L_a state reached after solvent rearrangement. PT is the proton-transfer state, corresponding to the excited conjugate anion ArO^-*, also of ^1L_a character, and the proton transferred to the solvent. The proton accepting base is supressed in the figure, for simplicity. The reaction coordinate is schematic, but at a minimum involves an important solvent component. The interconversion between the VB forms is discussed in the text. Note that two minima of the curve of PT/ArO^-* are drawn. The first one lies above that for the CT/^1L_a. This representation corresponds to the standard conditions, for which pH = 0 and $\Delta G_0 = RT\mathrm{p}K_a$* is positive. The second curve (dotted line) corresponds to high values of the pH, i.e., pH = 4.

alkaline solution, and the absorption to 3sPyO$^-$* (and subsequent fluorescence) recorded.

IV.4. Identification of the Intermediate in the ESPT Dynamics from 3sPyOH to Water. As indicated in the Introduction, one of the goals of the present work is to identify the nature of the excited states involved in the three-step kinetics of the proton-transfer reaction. From the above study of the solvatochromism of 3sPyOH, we have shown that, upon excitation of 3sPyOH, the ^1L_b state is reached and that its subsequent fate depends on the solvent−solute interaction. Under the influence of hydrogen bond interactions, the ^1L_b state relaxes toward the ^1L_a state, which becomes the fluorescing state. On the basis of the present study and the dynamics data,[15] we can now identify the locally excited (LE) state as the ^1L_b state whose solvation dynamics in water takes place within less than 300 fs.[15] We can also identify the mysterious intermediate state, to which LE converts within 2.2 ps, as the ^1L_a state with no proton-transfer involved.[15] In the final, third step, the ESPT occurs, converting the ^1L_a acid form to the 3sPyO$^-$* anion, *also* of ^1L_a character. The tentative connection with the three VB form model mentioned in the Introduction for the experimentally observed[15] three-step process is developed in the following section.

V. 3sPyOH in Water Intermediate in a Three-VB Form Perspective

The connection of the three step overall ESPT process with the three-VB form model could be the following. The first VB form would largely be a π* excited LE, without significant charge transfer from the oxygen lone pair of OH into the ring. In the language of the present work, this would be the dominant component of the ^1L_b state, accessed in absorption. The initial experimental fast step (<300 fs) would correspond to slight solvation dynamics as the solvent relaxes to equilibrium with the ^1L_b charge distribution, which is slightly different from that of the ground state. This first step is shown schematically in Figure 9. At this stage, the electronic character of the excited state has not changed.

The next step involves conversion to the second VB form, which would be characterized by significant charge transfer (CT) from the nonbonding orbital of O into the π* system, evidently including one or more of the SO_3^- groups in the 3sPyOH case. Due to its greater polarity than LE, the solvent rearrangement, including H-bondings through the OH and SO_3^- groups, is required in the conversion LE → CT, as indicated schematically in Figure 9. The CT VB form would then be a significant component of ^1L_a for solvation conditions ranging from those attained in the Franck−Condon absorption to those equilibrated to the CT form (Figure 9). Two points are important here. First, *no* PT has yet occurred. Second, the CT form/^1L_a intermediate is reached after the initial absorption (to LE/^1L_b) and requires solvent rearrangement with a certain time scale, which may involve either a slight solvent or proton coordinate barrier influenced by the coupling of the LE/^1L_b with the ^1L_a/CT state.[41,42] The second experimental time (2.2ps) is associated with this interconversion to form the intermediate, essentially the CT form. In view of the discussion in section IV.2 indicating that the ^1L_a/CT character is a strongly enhanced version of that present in ^1L_b, it would seem that the state inversion is a consequence of, or at least is assisted by, the response of the solvent to a polarity increase in the ^1L_b state compared to the ground state. The rearrangement of the solvent molecules and H-bond strengthening would serve to continually lower the energy of the ^1L_a state and ultimately to produce the locally stable ^1L_a state, whose equilibrated solvent configuration is quite different from the one originally reached in the Franck−Condon transition from the ground state and which produced ^1L_b. Internal vibronic coupling could well also play an important role in this state inversion process.[14,43] The basic dynamics just described for the second step in the overall 3sPyOH ESPT in water has much in common with those found in a simulation of excited-state 1-naphthol in water solvent by Knochenmuss et al.,[14] who stressed the solvent-induced level inversion after absorption to ^1L_b: one important difference is that the latter authors viewed such dynamics as those directly producing the proton-transferred products in that case.[44]

The final step, in VB language, is the proton-transfer step proper and would involve conversion between CT and the PT/VB form, which in the Mulliken picture[45] recently developed and supported for ground electronic state PT reactions,[9] would involve charge transfer from the nonbonding orbital of the base— here H_2O— into a σ* antibonding orbital of the OH-bond on the acid, inducing H motion toward the base, leading to the proton-transferred products. Note especially that this electronic rearrangment is *quite different* from transfer from the oxygen to the ring. Electronic coupling between the CT and PT/VB forms would produce the ^1L_a electronic state of the acid 3sPyOH and the anion 3sPyO$^-$, but both the composition of ^1L_a in terms of these two VB states and its energy vary as a function of the proton displacement and the solvent configurations, and in general will produce a barrier between the two limiting VB forms (Figure 9). This final interconversion between the CT and PT forms comprising the ^1L_a states of the acid and anion is governed in significant measure by the solvent reorganization and constitutes the third and final step of the proton transfer per se, associated with the third, long time scale (∼87 ps) in the 3sPyOH experiment in water.[46]

VI. Concluding Remarks

In this paper, we have addressed the issue of the intermediate state whose existence has been indicated by dynamic spectros-

copy experiments on ESPT for 3sPyOH in water.[15,17,18] To this end, we have studied the steady-state absorption and fluorescence, sulfonate substituent and solvent effects, and exploited quantum chemical calculations for ($3CO_2^-$) PyOH, as well as for the related compounds PyOH, pyrene, and carboxylated pyrenes. The major conclusions for the acids are the following. For PyOH, independent of the solvent, the absorption and fluorescence involve a ^1L_b state, with only very weak CT character. For 3sPyOH, absorption to a ^1L_b state is followed by an inversion to a ^1L_a state, from which fluorescence occurs. The latter ^1L_a state is characterized by significant CT character. The importance of the sulfonate groups in allowing the inversion was argued for, as was the stabilizing effect of hydrogen bonding to the solvent molecules. Based on the evidence and arguments presented, the intermediate state of 3sPyOH in water was identified as the ^1L_a state of the unionized acid, with significant CT character. As noted in the Introduction, previous discussions of $^1L_b/^1L_a$ inversion (for other hydroxyarene acids) have identified ^1L_a as the proton-transferred product state.[12,14]

A significant role in the interpretation of ^1L_a of the acid as an intermediate was played by the solvatochromism study of section IV, and it is of interest to consider related studies in the literature. In particular, we can compare our data with recent solvatochromism studies of 5-cyano-2-naphthol (5CN2NpOH).[47] These potentially provide a good comparison with our 3sPyOH study, since the cyano group generally displays an even more important electron-withdrawing character than the sulfonate group.[19] When the data of ref 47 is examined from the perspective of the present work, many strong similarities between the 5CN2NpOH and 3sPyOH properties can be discovered. First, the solvatochromism of the excited state on the absorption side is not pronounced; the variation of the absorption maximum, from the less to the most stabilizing solvent, is only 720 cm^{-1} (470 cm^{-1} for 3sPyOH). In contrast, on the fluorescence side, this variation becomes much larger (2560 cm^{-1}) for the same solvents (2210 cm^{-1} for 3sPyOH). As for 3sPyOH, the fitting of the fluorescence maxima as a function of the parameters of the solvents (eq I) shows high values of $s(\pi^*) = -1600$ and $b(\beta) = -1950$, which indicate an increased charge-transfer character. The role of the cyano group of 5CN2NpOH, as an electron-withdrawing substituent, seems however to be much weaker than that observed with the three SO_3^- of 3sPyOH: H-bond-donating solvents strongly stabilize 3sPyOH* but has no effect on 5CN2NpOH*. It would be interesting to perform quantum chemical calculations to provide a guide for the identification of the transitions of 5CN2NpOH, and to reexamine with a new eye the solvatochromism of the absorption and fluorescence bands, since this acid may provide a further example of intermediate state formation.

We close with several remarks on the relevance of the results of the present work for the more general question of current views of ESPT described in the Introduction.

The first remark concerns the traditional view that significant charge transfer is produced on excitation to the locally excited (LE) state, which would then be responsible for the enhanced excited-state acidity. The solvatochromism studies within indicate that while there is some CT character in the ^1L_b = LE state, the more significant CT character is indicated for the inverted ^1L_a states in all solvents, together with signatures of increased hydrogen bond donation to the solvents related to a weakened OH-bond in the acid. The first implication of this is that the traditional view that the significant CT occurs directly upon absorption requires modification. A second implication of this forms the basis of our second remark: inversion to ^1L_a after absorption, and the associated development of more pronounced CT character—i.e., the formation of the intermediate state— is necessary, but not sufficient, for kinetic ESPT to occur. In general, the conversion from the ^1L_b acid state to the ^1L_a acid state may or may not be facile, depending on the barrier and reaction free energetics for that step in Figure 9. Note that, in the more traditional $^1L_b/^1L_a$ state inversion scenario described in the Introduction, it is the height of any barrier associated with this step that would govern the rate of ESPT, as opposed to the present scenario for 3sPyOH, in which a ^1L_a intermediate acid form is produced. Certainly, it is possible that the effective barrier for the $^1L_b/^1L_a$ state inversion can be rate-limiting for the overall ESPT reaction in some cases.[14] We say only that this is not at all a universally valid situation for ESPT.

In our final remarks, we address the intrinsic proton-transfer step itself and return to the issue of the enhanced excited-state acidity. In this discussion, we focus on the 3sPyOH-type scenario in which a further, more substantial barrier for ESPT must be surmounted. In those cases where a locally stable intermediate acid form is produced on a time scale less than the excited-state lifetime, the next question would then be: what further features are critical in allowing the ESPT to take place during the lifetime of the excited state from a locally stable intermediate ^1L_a state which is evidently already "primed" for proton transfer in its charge redistribution and weakened OH-bond characteristics?

In our view, the answer to the question just posed is to be sought in the CT → PT kinetic barrier (Figure 9) that in general must be surmounted for ESPT to take place, and several aspects are likely to be important in determining that barrier (which, we again stress, is related to *different* electronic rearrangements in the Mulliken view (section V) than those associated with CT from the oxygen of OH into the ring.) First, based on a number of studies of ground-state acid−base proton-transfer reactions, a significant role should be played by the rearrangement of the solvent in connection with the evolving charge distribution associated with the displacement of the proton from the acid to the base.[9] Second, explicit attention to the role of the solvent stabilization, and indeed, the general energetics, of the excited-state *anion* seems to be required; for example, both general Bronsted barrier height-reaction free energy considerations[48,49] and Hammond postulate ideas[50] would suggest the importance of the anion to the reaction barrier height. In this connection, it is interesting to note that, in contrast with the focus on the reactant, acid, side in the ideas discussed within for proton transfer in the excited state, most discussions of *ground-state* acidity, e.g., in connection with substituent and solvent effects,[9,51,52] have focused on the anionic conjugate base side of the reaction. It would seem that an explanation of the enhanced excited-state acidity, as gauged by ΔpK_a values, as well as a comprehension of ESPT barrier heights, can only come when attention is paid to the product as well as the reactant side of an ESPT. Indeed, we have recently argued[41] via quantum chemistry calculations for phenol and cyanophenols that the enhanced excited-state acidity arises *not* from CT effects on the acid side of the reaction but rather from the much more important CT from oxygen into the ring for the *product anion*. As applied to 3sPyOH, this would suggest that while in the present study we have focused on the larger CT from oxygen into the ring in the ^1L_a state of the unionized acid compared to the locally excited ^1L_b state, the most important such CT would be present in the $3sPyO^-$ anionic product of the proton transfer. We plan to present a study on the solvatochromism of the

3sPyO$^-$ anion as well as a general discussion of ESPT including all the above features soon.

Acknowledgment. Two of the authors (T.-H. T.-T. and J.T.H.) acknowledge the support of an NSF-CNRS US-France International Collaboration grant. J.T.H. acknowledges support from the U. S. National Science Foundation Grant CHE 9700419, and a Research and Creative Work Faculty Fellowship (5/97-8/98) from the University of Colorado. The authors take this opportunity to express their appreciation for the many scientific contributions of Professor Mataga.

References and Notes

(1) Weller, A. *Z. Phys. Chem*. **1958**, *17*, 224.

(2) Weller, A. *Z. Elektrochem*. **1952**, *56*, 662. Avigal, I.; Feitelson, J.; Ottolenghi, M. *J. Chem. Phys*. **1969**, *50*, 2614. Rosenberg, J. L.; Brinn, I. *J. Phys. Chem*. **1972**, *76*, 3558.

(3) Arnaut, L. G.; Formosinho, S. J. *J. Photochem. Photobiol. A* **1993**, *75*, 1. Gutman, M.; Nachiel, E. *Biochim. Biophys. Acta*, **1990**, *1015*, 391.

(4) Förster, T. *Z. Elektrochem*. **1950**, *54*, 142. Jaffé, H. H.; Lloyd Jones, H. *J. Org. Chem*. **1965**, *30*, 1965. Grabowski, Z. R.; Grabowska, A. *Z. Phys. Chem. N. F. (Wiesbaden)* **1976**, *101*, 197. Grabowski, Z. R.; Rubaszewska, W. *J. Chem. Soc., Faraday Trans. 1* **1977**, *73*, 11. Robinson, G. W. *J. Phys. Chem*. **1991**, *95*, 10386. Wehry, E. L.; Rogers, L. B. *J. Am. Chem. Soc*. **1965**, *87*, 4234.

(5) For reviews, see: Barbara, P. F.; Walsh, P. K.; Brus, L. E. *J. Phys. Chem*. **1989**, *93*, 29. Syage, J. *J. Phys. Chem*. **1995**, *99*, 5772. See also the special issues: *J. Phys. Chem*. **1991**, *95*, 25; *Chem. Phys*. **1989**, *136*, 2; *Ber. Bunsen-Ges. Phys. Chem*. **1998**, *102*, 3.

(6) Vander Donckt, E. *Prog. React. Kinet*. **1961**, *1*, 187. Jackson, G.; Porter, G. *Proc. R. Soc.* **1961**, *A200*, 13. Dickens, P. G.; Linett, J. W. *Quart. Rev. Chem. Soc*. **1957**, *11*, 291. Salem, L. *Electrons in Chemical Reactions*; Wiley: New York, 1982.

(7) Mataga, N.; Kubota, T. *Molecular Interactions and Electronic Spectra*; Dekker: New York, 1970; Chapter 7.

(8) Bertran, J.; Chalvet, O.; Daudel, R. *Theor. Chim. Acta (Berlin)* **1969**, *14*, 1.

(9) Timoneda, J.; Hynes, J. T. *J. Phys. Chem*. **1991**, *95*, 10431. Staib, A.; Hynes, J. T.; Borgis, D. *J. Chem. Phys*. **1995**, *102*, 2487. Ando, K.; Hynes, J. T. *J. Phys. Chem*. **1997**, *101*, 10464. Ando, K.; Hynes, J. T. *J. Phys. Chem. A*, **1999**, *103*, 10398.

(10) For the different, albeit related, problem of proton transport in water, see the extensive references in: Marx, D.; Tuckerman, M. E.; Hutter, J.; Parinello, M. *Nature* **1999**, *397*, 601. Hynes J. T. *Nature* **1999**, *397*, 565.

(11) Platt, J. R. *J. Chem. Phys*. **1949**, *17*, 484.

(12) Tramer, A.; Zaborowska, M. *Acta Phys. Pol*. **1968**, *5*, 821.

(13) Knochenmuss, R.; Smith, D. E. *J. Chem. Phys*. **1994**, *101*, 7327.

(14) Knochenmuss, R.; Muiño, P. L.; Wickleder, C. *J. Phys. Chem*. **1996**, *100*, 11218. See also: Knochenmuss, R.; Fischer, I.; Luhus, D.; Lin, Q. *Isr. J. Chem*. **1999**, *39*, 221.

(15) Tran-Thi, T.-H.; Gustavsson, T.; Prayer, C.; Pommeret, S.; Hynes, J. T. *Chem. Phys. Lett*. **2000**, *329*, 421. Prayer, C.; Tran-Thi, T.-H.; Gustavsson, T. *AIP Conference Proceedings 364*; Tramer, A, Ed.; American Institute of Physics: New York, 1995; p 333.

(16) Pines, E.; Huppert, D. *Chem. Phys. Lett*. **1986**, *126*, 88. Pines, E.; Huppert, D.; Agmon, N. *J. Chem. Phys*. **1988**, *88*, 5620. See also: Genosar, L; Cohen, B.; Huppert, D. *J. Chem. Phys. A* **2000**, *104*, 6689.

(17) Prayer, C., Thesis 1997, UFR 926, University of Paris VI, Paris, France.

(18) Prayer, C.; Tran-Thi, T.-H.; Millié, Ph.; Hynes, J. T. *Abstract Book of the 18th International Conference On Photochemistry*; Polish Academy of Sciences: Warsaw, 1997.

(19) Jaffé, H. H. *Chem. Rev*. **1953**, *53*, 191. Taft, R. W.; Stanton Ehrenson, Jr.; Lewis, I. C.; Glick R. E. *J. Am. Chem. Soc*. **1959**, *81*, 5343. See also ref 36.

(20) Tietze, E.; Bayer, O. *Ann. Chem*. **1939**, *540*, 189.

(21) Velapoldi, R. A.; Mielenz, K. D. Standard Reference Materials: Fluorescence Standard Reference Material Quinine Sulfate Dihydrate; National Bureau of Standards, U. S. Department of Commerce, 1980; pp 260−64. Weber, G.; Teale, F. W. J. *Trans. Faraday Soc*. **1958**, *54*, 640.

(22) Momicchioli, F.; Baraldi, I.; Bruni, M. C. *Chem. Phys*. **1982**, *70*, 161.

(23) Szczepanski, J.; Vala, M.; Talbi, D.; Parisel, O.; Ellinger, Y. *J. Chem. Phys*. **1993**, *98*, 4494.

(24) Germain, A.; Millié, Ph., *Chem. Phys*. **1997**, *219*, 26.

(25) Marguet, S.; Germain, A.; Millié, Ph. *Chem. Phys*. **1996**, *208*, 351.

(26) Stewart, J. J. P.; Seiler, F. J. *MOPAC Program*, version 6.0; Research Laboratory, U. S. Air Force Academy: Colorado Springs, CO, 1989.

(27) Marguet, S.; Mialocq, J.-C.; Millié, Ph.; Berthier, G.; Momicchioli, F. *Chem. Phys*. **1992**, *160*, 265.

(28) Hoijting, G. J.; Velthorst, N. H.; Zandstra, P. J. *Mol. Phys*. **1960**, *3*, 533. Becker, R. S.; Sen Singh, I.; Jackson, E. A. *J. Chem. Phys*. **1963**, *38*, 2144.

(29) Thulstrup, E. W.; Downing, J. W.; Michl, J. *Chem. Phys*. **1977**, *23*, 307.

(30) Nakajima, A. *J. Lumin*. **1974**, *8*, 266.

(31) Stock, G.; Woywod, C.; Domcke, W.; Swinney, T.; Hudson, B. S. *J. Chem. Phys*. **1995**, *103*, 6851.

(32) Karpovich, D. S.; Blanchard, G. J. *J. Phys. Chem*. **1995**, *99*, 3951.

(33) Vasak, M.; Whipple, M. R.; Berg, A.; Michl, J. *J. Am. Chem. Soc*. **1978**, *100*, 6872.

(34) Note also that the oscillator strength of $S_0 \rightarrow {}^1L_b$ is greatly enhanced for 3sPyOH compared to PyOH, so that the oscillator strengths of the two transitions $S_0 \rightarrow {}^1L_b$ and $S_0 \rightarrow {}^1L_a$ have now become quantitatively comparable. This effect is not found with the calculations (Table 1), which predict instead that both the oscillator strengths would increase with the substitution of PyOH with the CO_2^- groups, but their ratio would remain the same ($(f({}^1L_a)/f({}^1L_b) = 8.3$) as that of the nonsubstituted compound. Apparently, despite the success described in the text for the CO_2^- modelling of the energy lowering effect of SO_3^- substitution, the perturbation of the charge distribution of such substitution is sufficiently great that the CO_2^- modelling fails for the oscillator strength ratio.

(35) On increasing the solvent polarity from toluene to chloroform to water, a weak blue shift is observed for the absorption band, 30 and 70 cm^{-1}, respectively. For the same solvents, a very weak red shift of -70 cm^{-1} is observed for the fluorescence band. These numbers are comparable to the estimated error bars of ± 63 cm^{-1} in this special wavelength domain.

(36) Baba, H.; Suzuki, S. *J. Chem. Phys*. **1961**, *35*, 1118.

(37) Bardez, E.; Goguillon, B. T.; Keh, E.; Valeur, B. *J. Phys. Chem*. **1984**, *88*, 1909.

(38) Wortmann, R.; Elich, K.; Lebus, S.; Liptay, W. *J. Chem. Phys*. **1991**, *95*, 6371.

(39) Kamlet, M. J.; Abboud, J.-L. M.; Abraham, M. H.; Taft, R. W. *J. Org. Chem*. **1983**, *48*, 2877. Marcus, Y.; Kamlet, M. J.; Taft, R. W. *J. Phys. Chem*. **1988**, *92*, 3613.

(40) Barrash-Shiftan, N.; Brauer, B. B.; Pines E. *J. Phys. Org. Chem*. **1998**, *11*, 743.

(41) Granucci, G.; Hynes, J. T.; Millié P.; Tran-Thi T.-H. *J. Am. Chem. Soc*. **2000**, *122*, 12243.

(42) As a parenthetical remark, we observe that it would have been interesting to study the solvatochomism behavior of ${}^1L_a$ in absorption, since one expects a stronger effect for ${}^1L_a$ which is more polar than ${}^1L_b$. However, it can be seen from Figure 6 that the position of the maximum of absorption corresponding to ${}^1L_a$ is completely hidden in the wide band which includes the two transitions. It is far from being clear whether the second peak of the absorption band would correspond to the maximum of absorption of the ${}^1L_a$ band. A clear example of the difficulty of deconvoluting these transitions is illustrated by the absorption and fluorescence spectra of 3sPyOH in EtOH (Figure 6).

(43) Kim, H. J.; Hynes, J. T. *J. Am. Chem. Soc*. **1992**, *114*, 10508. Kim, H. J.; Hynes, J. T. *J. Photochem. Photobiol. A* **1997**, *105*, 337.

(44) Another example of an inversion scenario of ${}^1L_b$ to ${}^1L_a$ without proton transfer is that proposed for 1-naphthol in Magnes, B.-Z.; Strashnikova, N. V.; Pines, E. *Isr. J. Chem*. **1999**, *39*, 361. There is however a difference between the present scenario and that of these authors. They found a wide and solvent-sensitive fluorescence band that they decomposed into two fluorescence bands assigned to the two simultaneously fluorescent ${}^1L_b$ and ${}^1L_a$ states. The two populations coexist but the relative percentage of ${}^1L_a$ increases with increasing polarity of the solvents. Such dual fluorescence is not observed for pyranine.

(45) Mulliken, R. S. *J. Phys. Chem*. **1952**, *56*, 801. *J. Chim. Phys*. **1964**, *60*, 20.

(46) In a recent experimental study of 3sPYOH in water solution containing 0.6 mol % glycerol over a wide temperature range [Poles, E.; Cohen, B. Huppert, D., *Isr. J. Chem.* **1999**, *39*, 347], an unusual non-Arrhenius temperature dependence is found. This was interpreted via a variant of a rate constant model for (electronically nonadiabatic) tunneling electron-transfer reactions [Rips, I.; Jortner, J., *J. Chim. Phys.-Chim. Biol.* **1987**, *87*, 2090. Hynes, J. T., *J. Phys. Chem*. **1986**, *90*, 3701.] to infer that there is only a very small barrier over and above any effect of solvent dynamics. While an equation of this general type has been discussed for (electronically adiabatic) proton-tunneling reactions [Borgis, D.; Hynes, J. T. *Chem. Phys.* **1993**, *170*, 315], in the absence of clear evidence for proton tunneling, a different approach (cf. ref 9b) could be more appropriate. This is under study.

(47) Solntsev, K. M.; Huppert, D.; Tolbert, L. M.; Agmon, N. *J. Am. Chem. Soc.* **1998**, *120*, 7981.

(48) Bronstead, J. N. *Chem. Rev.* **1928**, *5*, 231. Evans, M. G.; Polanyi, M. *Trans. Faraday Soc.* **1936**, *32*, 1340. Leffler, J. E. *Science* **1953**, *117*, 340.

(49) In this connection, see also: Pines, E.; Magnes, B.-Z.; Lang, M. L.; Fleming, G. R. *Chem. Phys. Lett.* **1997**, *281*, 413.

(50) Hammond, G. S. *J. Am. Chem. Soc.* **1955**, *77*, 334. Pross, A. *Adv. Phys. Org. Chem.* **1977**, *14*, 69.

(51) Fujio, M.; McIver, R. T.; Taft, R. W. *J. Am. Chem. Soc.* **1981**, *103*, 4017. McMahon, T. B.; Kebarle, P. *J. Am. Chem. Soc.* **1977**, *99*, 2222.

(52) Pauling, L. *The Nature Of The Chemical Bond*, Cornell University Press: Ithaca, NY, 1960. Pross, A.; Radom, L.; Taft, R. W. *J. Org. Chem.* **1980**, *45*, 818.